

<https://doi.org/10.1038/s41699-024-00506-4>

Mobility and threshold voltage extraction in transistors with gate-voltage-dependent contact resistance

Check for updates

Robert K. A. Bennett¹, Lauren Hoang¹, Connor Cremers¹, Andrew J. Mannix² & Eric Pop^{1,2,3} ✉

The mobility of emerging (e.g., two-dimensional, oxide, organic) semiconductors is commonly estimated from transistor current-voltage measurements. However, such devices often experience contact gating, i.e., electric fields from the gate modulate the contact resistance during measurements, which can lead conventional extraction techniques to estimate mobility incorrectly even by a factor >2 . Although this error can be minimized by measuring transistors at high gate-source bias $|V_{gs}|$, this regime is often inaccessible in emerging devices that suffer from high contact resistance or early gate dielectric breakdown. Here, we propose a method of extracting mobility in transistors with gate-dependent contact resistance that does not require operation at high $|V_{gs}|$, enabling accurate mobility extraction even in emerging transistors with strong contact gating. Our approach relies on updating the transfer length method (TLM) and can achieve $<10\%$ error even in regimes where conventional techniques overestimate mobility by $>2\times$.

The electron and hole mobilities of emerging semiconductors are frequently estimated from measured current vs. voltage characteristics (e.g., from drain current I_d vs. gate-source voltage V_{gs}) of field-effect transistors (FETs)¹. Many such transistors have contact resistance that is a function of gate voltage due to electrostatic gate fields that affect the energy barrier and charge density at the contact/channel interface^{2,3}. This *contact gating* effect is often associated with back-gated FETs (Fig. 1a), where the back gate can directly modulate the mobile charge carrier density at the contacts (Fig. 1b). However, recent work has shown that top-gated FETs (Fig. 1c) can also electrostatically control the contacts at their edges (Fig. 1d)^{4,5}.

Further complicating matters, the channel resistance R_{ch} and contact resistance R_C of contact-gated FETs often change at different rates (Fig. 1e), causing these devices to potentially exhibit two apparent threshold voltages: one associated with channel turn-on, and another dictated by contact turn-on⁶ (Fig. 1f). When the channel turns on before the contacts (i.e., at lower V_{gs} in *n*-channel FETs, as in Fig. 1e, f), I_d is limited by R_C and can remain low even when the channel is fully turned on (Fig. 1e, f, Region I). As V_{gs} increases, the contacts begin to turn on (Fig. 1e, f, Region II) before the device eventually reaches a channel-dominated regime (Fig. 1e, f, Region III), leading to a distinct kink⁷ in the I_d vs. V_{gs} characteristics associated with the transition between the contact- and channel-limited regimes.

Because I_d is contact-limited or contact-influenced in Region II of Fig. 1f, both I_d and the transconductance ($g_m = \partial I_d / \partial V_{gs}$) here are dominated by the contacts rather than by the channel. Thus, attempting to estimate the channel mobility (μ) using the conventional linear extrapolation method (i.e., asserting $\mu \propto g_m$) in this region can result in severe μ overestimation^{3,6-9} when R_C dominates and decreases as $|V_{gs}|$ increases. (In the special case where R_C remains constant as $|V_{gs}|$ increases, the mobility can be underestimated instead.) Therefore, μ should instead be extracted from the slope of Region III in Fig. 1f (where devices are channel-limited)^{7,8}. However, this approach is often infeasible for emerging semiconductor devices whose large R_C and/or early gate dielectric breakdown can make this high- $|V_{gs}|$ region hard to reach experimentally. Furthermore, when Region III of the I_d vs. V_{gs} curve is inaccessible before dielectric breakdown (e.g., due to large R_C and/or high threshold voltage $|V_T|$), the I_d vs. V_{gs} curve may show only a single linear region simply because the V_{gs} sweep ends early. For this reason, it can even be challenging to establish if a device is channel- or contact-limited based on its transfer characteristics¹⁰ alone.

To avoid μ overestimation due to contact gating, researchers can use four-terminal geometries to directly probe and subtract the voltage drop across the contacts^{9,11}. However, care must be taken to ensure that the voltage probes are entirely non-invasive, which can be difficult in practice¹²⁻¹⁵. The Y-function method¹⁶ can also correct for

¹Department of Electrical Engineering, Stanford University, Stanford, CA, USA. ²Department of Materials Science and Engineering, Stanford University, Stanford, CA, USA. ³Department of Applied Physics, Stanford University, Stanford, CA, USA. ✉e-mail: epop@stanford.edu

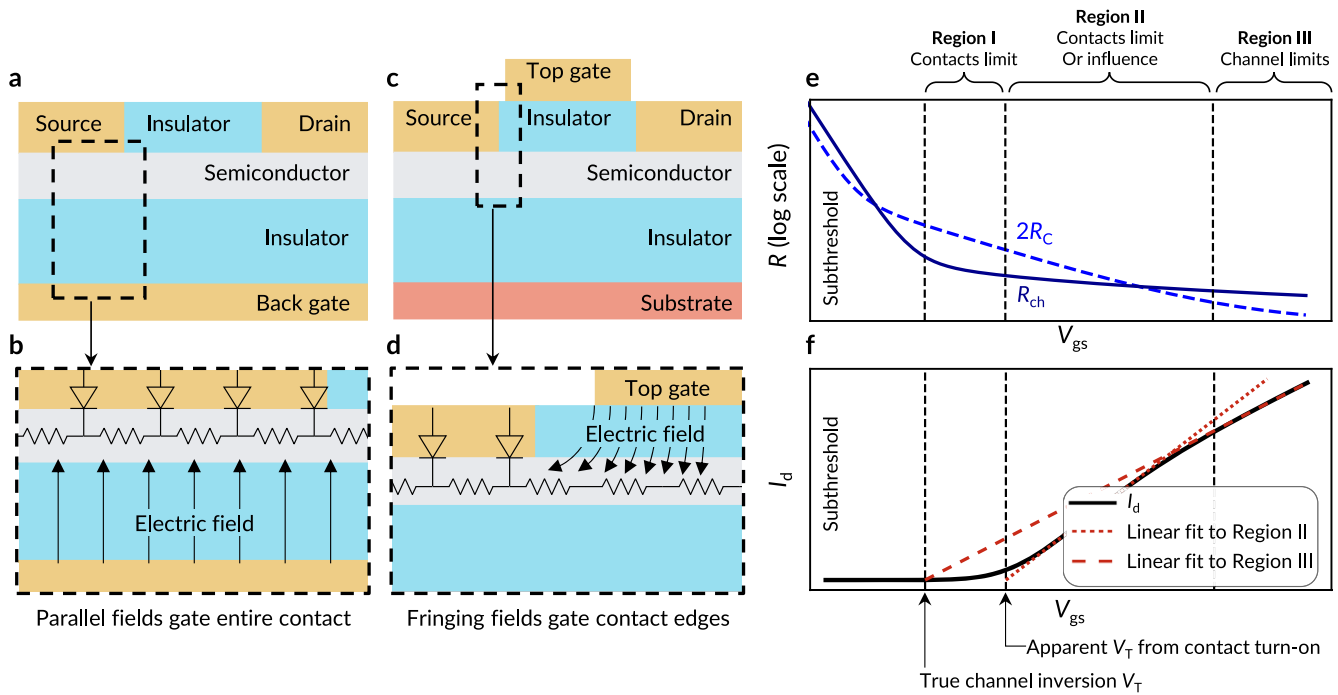


Fig. 1 | Contact gating in field-effect transistors (FETs). **a** Schematic of a back-gated FET, where inset **b** shows the parallel field from the back gate directly gating the entire contact. **c** Schematic of a top-gated FET, where inset **d** shows fringing fields gating the contact edge. (Top-gated devices without underlaps would have their contact edges gated directly by the parallel field instead.) As a result of contact gating, the channel resistance R_{ch} and contact resistance R_C can decrease at different rates as V_{gs} increases (**e**), creating a distinct kink in the resultant I_d vs. V_{gs} characteristics (**f**). After exiting the subthreshold region, the channel may turn on even as the contacts

remain off, suppressing I_d (**e, f**, Region I). The contacts then turn on as V_{gs} further increases, leading to a sharp increase of I_d (**e, f**, Region II). The magnitude and slope of I_d here are dictated by the contacts rather than by the channel; attempting to extract the channel mobility from this region with conventional techniques can result in severe overestimation. Finally, the FET returns to a channel-limited regime when $2R_C < R_{ch}$ (**e, f**, Region III); μ can usually be safely extracted from this region. The diagrams shown here are for an n -channel FET.

mild contact gating¹⁷ but relies upon accurate V_T extraction, making this method unreliable for devices that cannot access Region III⁶ in Fig. 1f. We demonstrate later in this work that the transfer length method (TLM) approach¹ can be similarly unreliable for extracting μ from contact-gated FETs.

In this work, we propose a method for extracting the channel μ and V_T of transistors that remains valid even for strongly contact-gated devices. This approach takes inspiration from the conventional TLM method¹ and can analyze families of two-terminal devices that cannot access the channel-limited regime (Fig. 1e, f, Region III) in their I_d vs. V_{gs} measurements. We validate our proposed method using synthetic data generated by a technology computer-aided design (TCAD) simulator¹⁸ and find that it accurately extracts μ even for devices where conventional methods overestimate μ by 2–3 \times , enabling accurate μ and V_T extraction in devices with strong contact gating.

Results

Our proposed extraction is summarized in Fig. 2 and explained in detail below. We provide Python code to automate this extraction in a GitHub Repository¹⁹ and in Supplementary Section 4. Additionally, we provide a tutorial for this code in Supplementary Section 1.

Model derivation

Here, we treat a contact-gated FET as a channel between gate-voltage-dependent source and drain resistors (R_s and R_d respectively); the total contact resistance is $2R_C = R_s + R_d$, as shown in Fig. 2a²⁰. The intrinsic gate-to-source and drain-to-source biases (after considering the voltage drops across R_s and R_d) are $V'_{gs} = V_g - V'_s$ and $V'_{ds} = V'_d - V'_s$, where V'_s and V'_d are defined in Fig. 2a. In the linear region of an n -channel FET ($V'_{gs} > V_T$

and $V'_{ds} < V'_{gs} - V_T$), I_d is:

$$\frac{I_d}{W} = \frac{\mu C_{ox}}{L_{ch}} \left(V'_{gs} - V_T - \frac{V'_{ds}}{2} \right) V'_{ds} \tag{1}$$

where C_{ox} is the gate insulator capacitance per unit area, and W and L_{ch} are the width and length of the channel. In this extraction, we build a system of equations based on Eq. (1) that we use to simultaneously solve for μ and V_T . In Eq. (1), V_T refers explicitly to the true channel V_T associated with channel inversion (as defined in Fig. 1f); thus, this channel V_T often cannot be extracted directly in contact-gated devices. [For emerging FETs with intrinsic channels (no counter-doping), such as two-dimensional (2D) FETs, the channel is considered inverted when the carrier concentration is approximately equal to the density of states at the relevant band edge²¹.]

To build our system of equations, we use a TLM-like approach where we consider a family of devices with various L_{ch} (using multiple two-terminal devices or a larger TLM-like test structure). As R_s and R_d are V_{gs} -dependent, we use I_d vs. V_{ds} sweeps at fixed values of V_{gs} to ensure these resistances remain constant. Further, as R_s and R_d contain Schottky diodes, they are nonlinear circuit elements, i.e., their resistances are functions of I_d . To ensure constant R_C , we therefore perform the extraction at a constant current.

With these considerations in mind, we begin by choosing a target drain current I_d^T . We then perform I_d vs. V_{ds} sweeps for each L_{ch} at a common V_{gs} , recording the V_{ds} at which the device with the i^{th} channel length reaches $I_d = I_d^T$ as $V_{ds} = V_{ds}^{(i)}$ (Fig. 2b). Then, we plot $V_{ds}^{(i)}$ vs. L_{ch} and perform linear regression (Fig. 2c); the y -intercept of the line of best fit yields the voltage drop across the contacts ΔV_C at $I_d = I_d^T$. (ΔV_C is the summed voltage drop

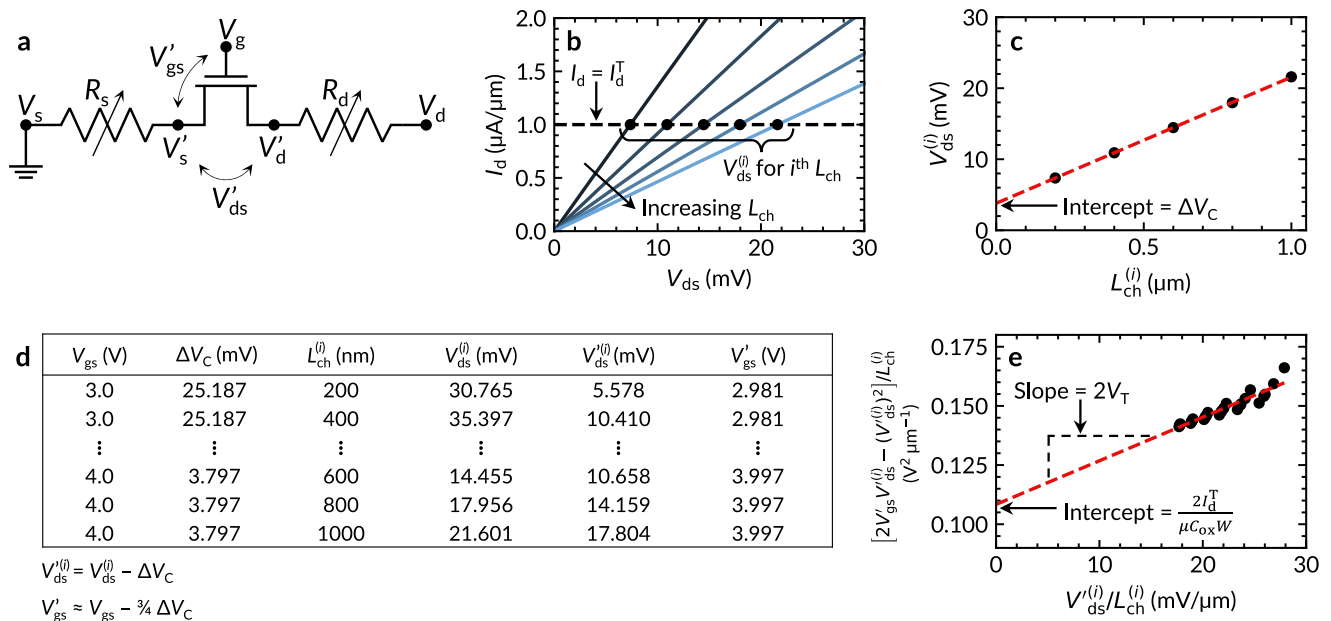


Fig. 2 | Summary of our proposed extraction. We treat a contact-gated FET as a channel between gate-voltage-dependent contact resistors (a). We begin the extraction in b by performing I_d vs. V_{ds} sweeps at a fixed V_{gs} for a family of devices with varying channel lengths L_{ch} . For the i^{th} L_{ch} , we record the V_{ds} at which the drain current reaches a target drain current $I_d = I_d^T$ as $V_{ds} = V_{ds}^{(i)}$. We then plot $V_{ds}^{(i)}$ vs. L_{ch} in c and extrapolate to find the voltage drop across the contacts ΔV_C . We repeat this

procedure at multiple V_{gs} to compile the table in d (using the equations below the table to calculate the intrinsic voltages). Finally, we use data from d to prepare the plot shown in e, perform linear regression to find the slope m and y -intercept b , and extract $V_T = m/2$ and $\mu = 2I_d^T/(bC_{ox}W)$. We use the Monte Carlo approach described in Supplementary Section 2 to propagate error throughout the extraction in order to improve the accuracy of the extraction and to estimate standard error.

across the source and drain contacts, not the average voltage drop across either contact.) Here, I_d^T must be chosen such that the extracted $V_{ds}^{(i)}$ values are small (all $V_{ds}^{(i)} \ll V_{gs} - V_T$) to minimize the quadratic term in Eq. (1); otherwise, the linear fit in Fig. 2c becomes invalid. Additionally, a small $V_{ds}^{(i)}$ ensures that the vertical electric field near the drain is similar for all channel lengths, helping to ensure that R_d remains constant across all devices.

Next, we partition ΔV_C into the voltage drops across the source and drain, ΔV_s and ΔV_d . As R_s and R_d contain reverse- and forward-biased Schottky diodes, respectively, we have $R_s > R_d$ ²⁰. Further, as R_d approaches 0 for high drain bias²², we have:

$$0 \leq \Delta V_d \leq \Delta V_C/2 \tag{2}$$

$$\Delta V_C/2 \leq \Delta V_s \leq \Delta V_C \tag{3}$$

For simplicity, we take the centers of these ranges, i.e., $\Delta V_d \approx \frac{1}{4} \Delta V_C$ and $\Delta V_s \approx \frac{3}{4} \Delta V_C$, and estimate the true intrinsic voltages as $V_{ds}^{(i)} = V_{ds}^{(i)} - \Delta V_C$ and $V_{gs}' = V_{gs} - \Delta V_s \approx V_{gs} - \frac{3}{4} \Delta V_C$.

We use the above approach to extract $V_{ds}^{(i)}$ and V_{gs}' at multiple fixed V_{gs} values to compile the table in Fig. 2d. Next, we use these tabulated values to build a system of equations from which we extract μ and V_T . To do so, we rearrange Eq. (1) into:

$$\frac{2V_{gs}'V_{ds}^{(i)} - V_{ds}^{(i)2}}{L_{ch}} = 2V_T \frac{V_{ds}^{(i)}}{L_{ch}} + \frac{2I_d}{\mu C_{ox}W} \tag{4}$$

As Eq. (4) is in the form $y = mx + b$ [with $m = 2V_T$, $x = V_{ds}^{(i)}/L_{ch}$, and $b = 2I_d/(\mu C_{ox}W)$], we use rows from Fig. 2d to plot $(2V_{gs}'V_{ds}^{(i)} - V_{ds}^{(i)2})/L_{ch}^{(i)}$ as a function of $V_{ds}^{(i)}/L_{ch}^{(i)}$ and perform linear regression (Fig. 2e). We then use the extracted slope and intercept to calculate V_T and μ from known quantities.

Although we present this derivation for n -type devices, this procedure can easily be adapted to p -type devices by repeating the derivation starting from the p -type analog of Eq. (1). Alternatively, one could apply the above procedure to p -type devices by negating the input V_{gs} , taking the absolute value of V_{ds} , and then negating the extracted V_T .

We note that ΔV_C extracted in Fig. 2c is accompanied by an associated error that leads to uncertainty in the extracted μ and V_T . Simple analytic techniques cannot easily propagate this error to the final estimated μ and V_T because the quantities along both the x - and y -axes in Fig. 2e are error-prone, where the errors in x and y values are not mutually independent. Hence, we instead use the Monte Carlo approach described in Supplementary Section 2 to propagate this error, allowing us to improve the estimates for the nominal μ and V_T and their standard errors. This Monte Carlo approach is implemented in Python code that we provide in Supplementary Section 4 and in an online GitHub Repository¹⁹.

Model validation

We validate our proposed extraction by using it to estimate μ and V_T from current-voltage characteristics generated by Sentaurus Device TCAD¹⁸. This approach allows us to assess the accuracy of the extraction because μ and V_T are known a priori: μ is a simulation input parameter, and the channel V_T can be extracted from equivalent devices (simulated in Sentaurus) without contact resistance.

The contact-gated devices in our TCAD simulations have nominal Schottky barrier heights $\phi_B = 0.15, 0.3, 0.45,$ and 0.6 eV. These are “nominal” values because the TCAD simulations include image force lowering (IFL)²³ and tunneling at the contacts; these listed ϕ_B are barrier heights before IFL (i.e., the ϕ_B we list are the differences between the semiconductor’s electron affinity and the metal’s work function). All devices are back-gated transistors (Fig. 1a) with HfO₂ gate insulators (relative dielectric constant $\kappa = 20$ and equivalent oxide thickness EOT = 10 nm). The channel thickness is 0.615 nm (corresponding to monolayer MoS₂^{24,25}) and the mobility is set to $\mu = 50$ cm²V⁻¹s⁻¹.

In Fig. 3a–d, we plot TCAD-generated I_d vs. V_{ov} sweeps (where the overdrive voltage $V_{ov} = V_{gs} - V_T$) at $V_{ds} = 0.1$ V for each ϕ_B at $L_{ch} = 200, 400, \dots, 1000$ nm. Devices with $\phi_B \geq 0.3$ eV clearly display the signature kink

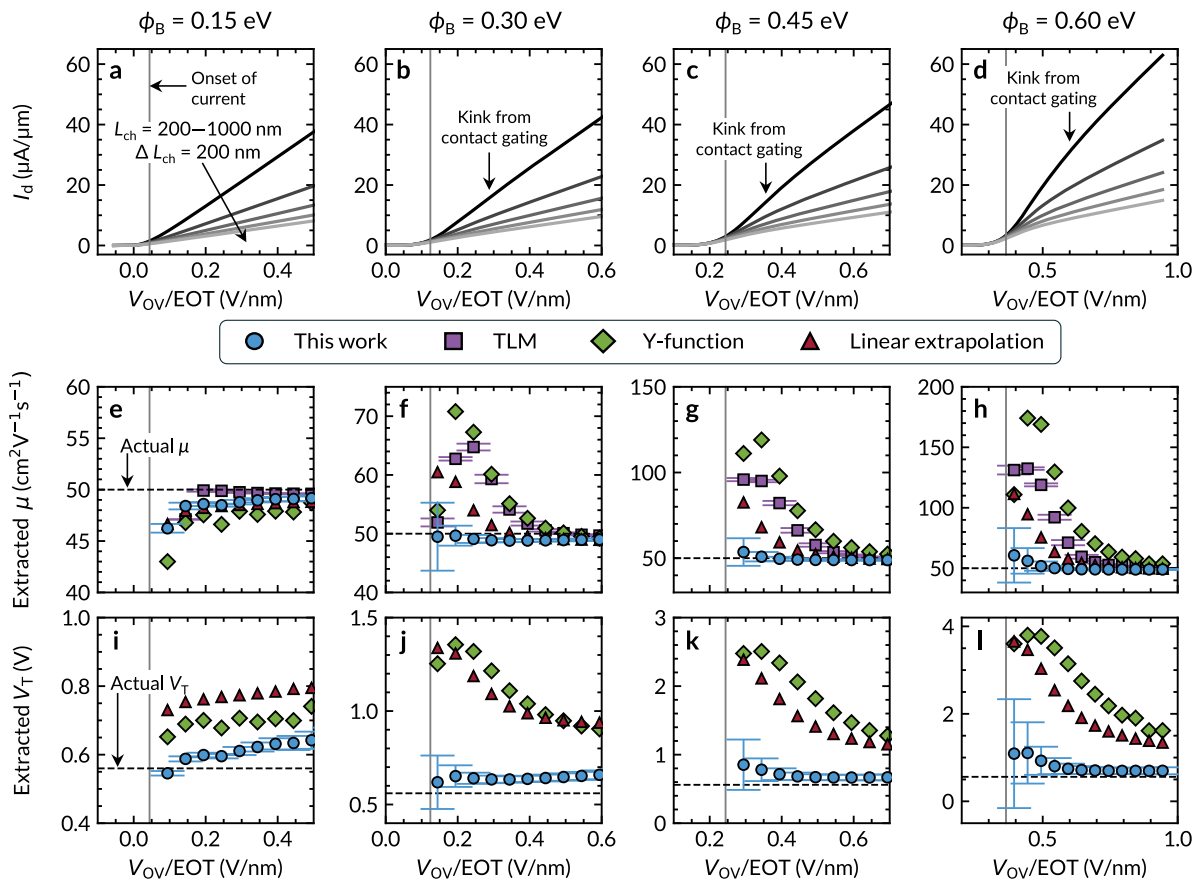


Fig. 3 | Validation of our proposed extraction. I_d vs. V_{ov} for families of devices with $L_{ch} = 200, 400, \dots, 1000$ nm and Schottky barrier height $\phi_B =$ **a** 0.15 eV, **b** 0.3 eV, **c** 0.45 eV, and **d** 0.6 eV. x -axes show different ranges of V_{ov}/EOT to highlight device characteristics and extractions near I_d turn-on for different ϕ_B . Solid gray lines mark the approximate I_d turn-on for each device family. **e** The mobility μ extracted with our method and the linear extrapolation, Y-function, and TLM approaches for

device families with $\phi_B = 0.15$ eV, **f** 0.3 eV, **g** 0.45 eV, and **h** 0.6 eV plotted vs. V_{ov}/EOT . Horizontal dashed lines mark the true μ . The x -axes are the same as in **i-l**. The threshold voltage V_T extracted with each method for device families with $\phi_B = 0.15$ eV, **j** 0.3 eV, **k** 0.45 eV, and **l** 0.6 eV plotted vs. V_{ov}/EOT . The horizontal dashed lines mark the true channel V_T .

of contact gating⁷ (especially at small L_{ch} , where R_C exceeds the channel resistance at low V_{ov}). Next, we plot the extracted μ and V_T for each ϕ_B using our proposed extraction method and three conventional techniques: the linear extrapolation, Y-function, and TLM approaches^{1,16,26}. These conventional techniques are applied directly on the synthetic I_d vs. V_{gs} data shown in Fig. 3a–d, whereas our extraction uses separate synthetic I_d vs. V_{ds} data. The linear extrapolation and Y-function techniques both use the device with the longest channel ($L_{ch} = 1000$ nm), whereas our proposed method and the TLM approach use the full range of $L_{ch} = 200$ –1000 nm in Fig. 3a–d. We calculate standard error using the method described in Supplementary Section 2 for our proposed extraction method, and we use the standard error from linear regression (equivalent to the 68% confidence interval) for the TLM approach. (We do not include standard error for the linear extrapolation or Y-function approaches because the synthetic data is noiseless.)

In Fig. 3e–h, we plot the μ extracted from each method vs. V_{ov}/EOT . The horizontal axes in these plots are shown only up to the point where the μ obtained by the four extraction methods have converged. At $\phi_B = 0.15$ eV (Fig. 3e), we find that all extractions yield reasonable estimates for μ , with a worst-case underestimation of $\sim 15\%$ for the Y-function method. As ϕ_B increases, however, we find that conventional methods begin to severely overestimate μ due to contact gating. We also note the TLM approach predicts a small standard error ($<10\%$) in Fig. 3g, h ($\phi_B = 0.45$ and 0.6 eV) despite overestimating μ by over 2 \times . In other words, the standard error estimated from the TLM approach does not accurately reflect the true uncertainty in the extracted μ when ϕ_B is large and V_{ov} is limited (e.g., by early dielectric

breakdown). In contrast, our method estimates μ more accurately than conventional methods, with a worst-case overestimation of $\sim 20\%$ at $\phi_B = 0.6$ eV and low V_{ov} (Fig. 3h), and with the true μ being captured within our error bars (unlike the TLM method).

We note that the TLM approach requires that devices with different L_{ch} be measured at a common carrier density, i.e., at a common V_{ov} ¹. In the present work, V_{ov} is referenced with respect to the V_T estimated by linear extrapolation; in Supplementary Section 3, we study the accuracy of the TLM approach when instead using V_T defined at a constant current (e.g., 100 nA/ μm).

Next, in Fig. 3i–l, we plot the V_T extracted from our proposed method, the linear extrapolation method, and the Y-function method vs. V_{ov}/EOT using the same horizontal x -axis limits as in Fig. 3e–h. Importantly, in these transistors, contact gating obscures the channel turn-on, causing the linear extrapolation and Y-function methods to significantly overestimate V_T . In comparison, we find that our proposed extraction tends to yield much more accurate V_T estimates, with a worst-case V_T error of 0.2 V in the range of V_{ov}/EOT plotted in Fig. 3i–l. We note that our method and the conventional methods tested here do not always converge to the true V_T at higher V_{ov} , but this is acceptable because the error in estimated V_T is less impactful (i.e., has smaller impact on the predicted charge carrier density) at large V_{ov} .

To ensure that our proposed extraction is applicable to a variety of devices (and not limited to those presented in Fig. 3), we repeat similar extractions for back-gated transistors with (i) $\mu = 5$ cm²V⁻¹s⁻¹ and EOT = 10 nm and (ii) $\mu = 50$ cm²V⁻¹s⁻¹ and EOT = 100 nm (channel

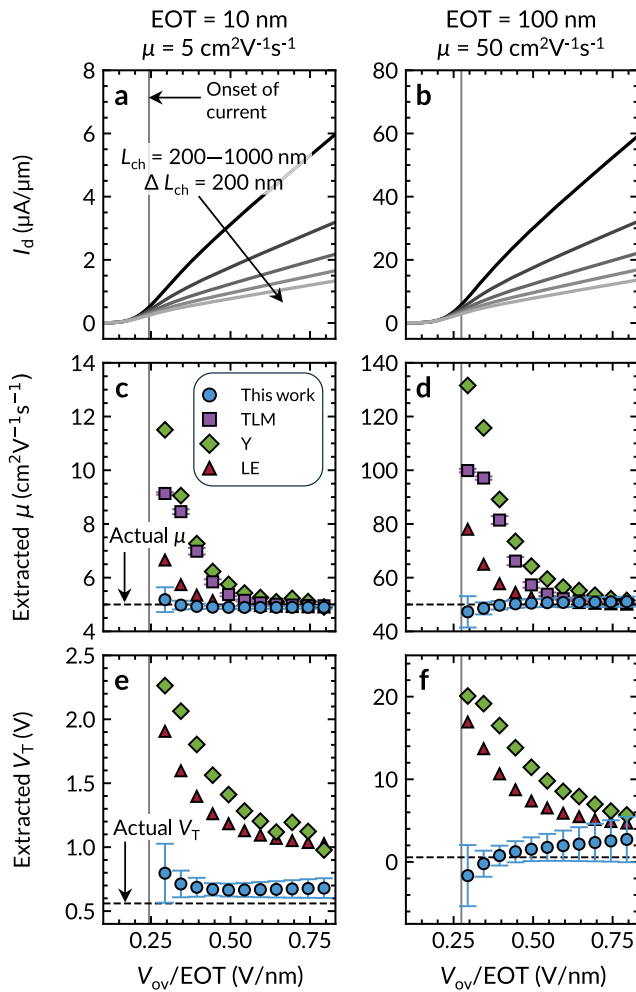


Fig. 4 | Validation of our proposed extraction on low-mobility and high-EOT transistors. I_d vs. V_{ov} for families of devices with $L_{ch} = 200, 400, \dots, 1000$ nm and Schottky barrier height $\phi_B = 0.45$ eV with **a** EOT = 10 nm and mobility $\mu = 5 \text{ cm}^2\text{V}^{-1}\text{s}^{-1}$ and **b** EOT = 100 nm and $\mu = 50 \text{ cm}^2\text{V}^{-1}\text{s}^{-1}$. The solid gray lines mark the approximate I_d turn-on for each family of devices, and the x-axes are the same as in **c**, **d** and **e**, **f**. **c** The extracted mobility μ with our method and the linear extrapolation (LE), Y-function (Y), and TLM approaches for device families with EOT = 10 nm and mobility $\mu = 5 \text{ cm}^2\text{V}^{-1}\text{s}^{-1}$ and **d** EOT = 100 nm and $\mu = 50 \text{ cm}^2\text{V}^{-1}\text{s}^{-1}$ plotted vs. V_{ov}/EOT . The horizontal dashed line marks the true μ . **e** The threshold voltage V_T extracted with each method for devices with EOT = 10 nm and $\mu = 5 \text{ cm}^2\text{V}^{-1}\text{s}^{-1}$ and **f** EOT = 100 nm and $\mu = 50 \text{ cm}^2\text{V}^{-1}\text{s}^{-1}$. Horizontal dashed lines mark the true channel V_T .

thickness = 0.615 nm and $\phi_B = 0.45$ eV for all devices) in Fig. 4. These scenarios are relevant because they correspond to typical devices used to test emerging semiconductor channels. We plot I_d vs. V_{ov} in Fig. 4a, b, extracted μ in Fig. 4c, d, and extracted V_T in Fig. 4e, f. We find that the trends observed here are similar to those of Fig. 3, suggesting that our proposed extraction remains applicable at higher EOTs or lower μ . Thus, the method we propose in this work appears to facilitate accurate extractions from a variety of contact-gated transistors with high R_C and/or early dielectric breakdown that cannot access the higher V_{ov} range necessitated by conventional methods.

Effect of device-to-device variation

To assess the robustness of our extraction, we apply it to devices whose μ and V_T have a certain amount of variation, as would be seen experimentally. For each device, we randomly select μ and V_T

according to Gaussian distributions with means (standard deviations) of $50 \text{ cm}^2\text{V}^{-1}\text{s}^{-1}$ (10%) and 0.56 V (0.1 V), respectively. As before, we use Sentaurus TCAD¹⁸ to generate current-voltage characteristics that we analyze with our proposed method and the TLM approach. Because the Y-function and linear extrapolation methods are applied to one device at a time, they are not affected by variations between devices; thus, we do not re-analyze them here. We quantify each method’s accuracy in terms of its mean absolute error (MAE) and its confidence interval coverage probability (CICP; the probability that the true μ lies within the range of estimated value \pm the error). In other words, an MAE near 0% (or as small as possible) and a CICP close to 100% (or as large as possible) are desirable. All devices are identical to those used in Fig. 3c, i.e., back-gated with EOT = 10 nm, channel thickness = 0.615 nm, and $\phi_B = 0.45$ eV.

We perform 100 extractions on families of devices with 5 channel lengths ($L_{ch} = 200, 400, \dots, 1000$ nm), starting at high $V_{ov}/EOT = 0.64$ V/nm. We find that our proposed approach and the TLM approach offer reasonably small MAE = 14.3% and 10.9% (on the same order as the μ standard deviation), respectively, and CICPs of 99% and 65%, respectively (Fig. 5a, b), indicating that random variation does not significantly affect the accuracy or reliability of these methods at high V_{ov} .

Next, we repeat this procedure at smaller $V_{ov}/EOT = 0.3$ V/nm, which lies within the contact-influenced region of the I_d vs. V_{ov} curves in Fig. 3c. Here, the MAE of our proposed method increases to 20.2% and its CICP remains high at 94% (Fig. 5c). However, the MAE of the TLM approach increases greatly to 116.0% (>2× mobility overestimation), whereas its CICP falls to 0%, i.e., the TLM approach did not estimate μ to within error bars across any of the 100 trials (Fig. 5d). The MAE of our approach can be improved by adding more devices; repeating the extraction at $V_{ov}/EOT = 0.3$ V/nm using three of each L_{ch} (Fig. 5e; with devices subject to the same random variations as before) decreases the MAE of our approach to 13.3%, though the CICP also worsens slightly to 78% (which may occur in part because the estimated standard error shrinks). However, the MAE of the TLM approach only decreases slightly to 110.0% (~2× mobility overestimation) and the CICP remains at 0% (Fig. 5f), indicating that adding more devices to the TLM analysis is ineffective for improving both accuracy and reliability at $V_{ov}/EOT = 0.3$ V/nm.

We note that although Fig. 5c shows our method yields a reasonably low MAE = 20.2% on the entire set of 100 device families, the 10 worst extractions still overestimate μ by 48% to 102%. However, the CICP considering only these 10 extractions is 100%, i.e., each of these 10 worst extractions also yielded large estimated errors that encompassed the true μ of $50 \text{ cm}^2\text{V}^{-1}\text{s}^{-1}$. Thus, although our method can overestimate μ of contact-gated devices (here with $\phi_B = 0.45$ eV), these overestimations are accompanied by large error bars that clearly indicate when the extraction is error-prone.

Discussion

We have developed a simple method for extracting the mobility and channel threshold voltage from transistors with gate-voltage-dependent contact resistance. We tested this method by analyzing TCAD-generated current-voltage characteristics and showed it can accurately extract the mobility and threshold voltage when devices are heavily influenced by contact gating, even when conventional methods overestimate the mobility by 2–3×. We also find that the standard error associated with the estimated mobility and threshold voltage tends to accurately reflect the actual uncertainty in the extraction, enabling a high confidence extraction of mobility even in regimes where the TLM approach fails. Hence, our method expands the range of overdrive voltages that can be used to estimate mobility and threshold voltage, allowing these quantities to be more accurately determined in emerging semiconductor devices with high contact resistance and/or early dielectric breakdown.

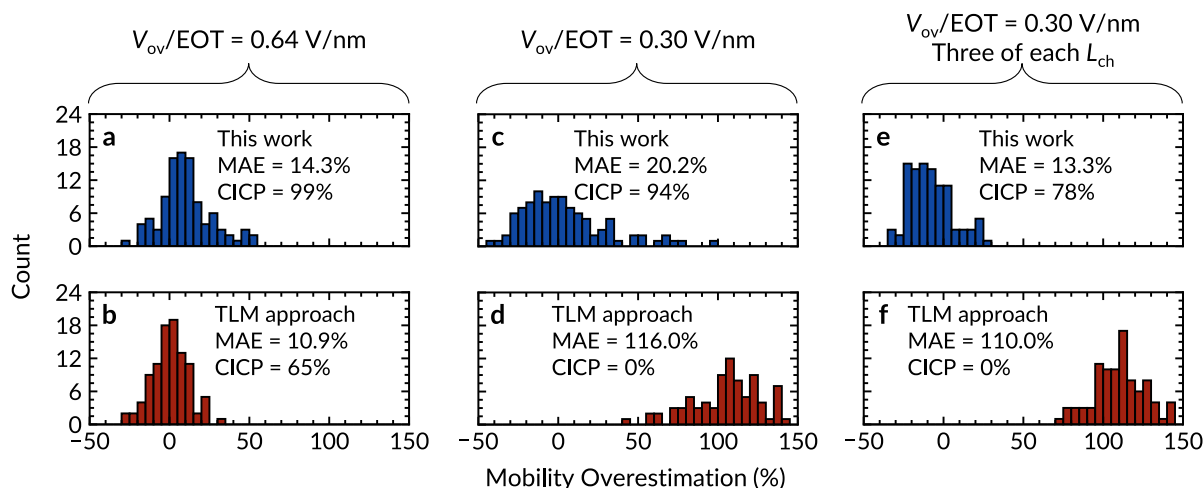


Fig. 5 | Robustness to variation of our method and of the TLM approach. Histograms of mobility overestimations for 100 families of devices with $L_{ch} = 200, 400, \dots, 1000$ nm. The devices are selected at random from a Gaussian distribution with mean (standard deviation) $\mu = 50 \text{ cm}^2 \text{ V}^{-1} \text{ s}^{-1}$ (10%) and mean (standard deviation) $V_T = 0.56 \text{ V}$ (0.1 V). **a** Our method and **b** the TLM approach at high $V_{ov}/EOT =$

0.64 V/nm. **c** Our method and **d** the TLM approach at lower $V_{ov}/EOT = 0.3 \text{ V/nm}$. **e** Our method and **f** the TLM approach at $V_{ov}/EOT = 0.3 \text{ V/nm}$ with three of each L_{ch} used in the extraction. Each figure lists the mean absolute error (MAE, ideally should be close to 0%) and confidence interval coverage probability (CICP, ideally should be close to 100%).

Data availability

The datasets used and/or analysed during the current study available from the corresponding author on reasonable request.

Code availability

Code that automates the extraction proposed in this work is included in Supplementary Section 4 and in an online GitHub repository¹⁹.

Received: 15 June 2024; Accepted: 19 September 2024;

Published online: 17 February 2025

References

- Cheng, Z. et al. How to report and benchmark emerging field-effect transistors. *Nat. Electron.* **5**, 416–423 (2022).
- Arutchelvan, G. et al. From the metal to the channel: a study of carrier injection through the metal/2D MoS₂ interface. *Nanoscale* **9**, 10869–10879 (2017).
- Prakash, A., Ilatikhameneh, H., Wu, P. & Appenzeller, J. Understanding contact gating in Schottky barrier transistors from 2D channels. *Sci. Rep.* **7**, 12596 (2017).
- Alharbi, A. & Shahrjerdi, D. Analyzing the effect of high-k dielectric-mediated doping on contact resistance in top-gated monolayer MoS₂ transistors. *IEEE Trans. Electron Devices* **65**, 4084–4092 (2018).
- Ber, E., Grady, R. W., Pop, E. & Yalon, E. Uncovering the different components of contact resistance to atomically thin semiconductors. *Adv. Electron. Mater.* **9**, 2201342 (2023).
- Nasr, J. R., Schulman, D. S., Sebastian, A., Horn, M. W. & Das, S. Mobility deception in nanoscale transistors: an untold contact story. *Adv. Mater.* **31**, 1806020 (2019).
- McCulloch, I., Salleo, A. & Chabinyk, M. Avoid the kinks when measuring mobility. *Science* **352**, 1521–1522 (2016).
- Bittle, E. G., Basham, J. I., Jackson, T. N., Jurchescu, O. D. & Gundlach, D. J. Mobility overestimation due to gated contacts in organic field-effect transistors. *Nat. Commun.* **7**, 10908 (2016).
- Pang, C.-S. et al. Mobility extraction in 2D transition metal dichalcogenide devices—avoiding contact resistance implicated overestimation. *Small* **17**, 2100940 (2021).
- Liu, C. et al. Device physics of contact issues for the overestimation and underestimation of carrier mobility in field-effect transistors. *Phys. Rev. Appl.* **8**, 034020 (2017).
- Mitta, S. B. et al. Electrical characterization of 2D materials-based field-effect transistors. *2D Mater.* **8**, 012002 (2021).
- English, C. D., Shine, G., Dorgan, V. E., Saraswat, K. C. & Pop, E. Improved contacts to MoS₂ transistors by ultra-high vacuum metal deposition. *Nano Lett.* **16**, 3824–3830 (2016).
- Ng, H. K. et al. Improving carrier mobility in two-dimensional semiconductors with rippled materials. *Nat. Electron.* **5**, 489–496 (2022).
- Wu, P. Mobility overestimation in molybdenum disulfide transistors due to invasive voltage probes. *Nat. Electron.* **6**, 836–838 (2023).
- Ng, H. K. et al. Reply to: Mobility overestimation in molybdenum disulfide transistors due to invasive voltage probes. *Nat. Electron.* **6**, 839–841 (2023).
- Jin, H., Xing, Z., Yangyuan, W. & Ru, H. New method for extraction of MOSFET parameters. *IEEE Electron Device Lett.* **22**, 597–599 (2001).
- Chang, H.-Y., Zhu, W. & Akinwande, D. On the mobility and contact resistance evaluation for transistors based on MoS₂ or two-dimensional semiconducting atomic crystals. *Appl. Phys. Lett.* **104**, 113504 (2014).
- Synopsys Inc., Sentaurus Device. (Sunnyvale CA, USA, 2017).
- Bennett, R. K. A. *GitHub Repository*. Available online: github.com/RKABennett/VT_mu_extraction.
- Chiquito, A. J. et al. Back-to-back Schottky diodes: the generalization of the diode theory in analysis and extraction of electrical parameters of nanodevices. *J. Phys. Condens. Matter* **24**, 225303 (2012).
- Lundstrom, M. S. *Fundamentals of Nanotransistors*. Chapter 9.4: The Mobile Charge: Extremely Thin SOI; The Mobile Charge Below Threshold. (World Scientific Publishing, 2015).
- Nipane, A., Teherani, J. T. & Ueda, A. Demystifying the role of channel region in two-dimensional transistors. *Appl. Phys. Express* **14**, 044003 (2021).
- Vaknin, Y., Dagan, R. & Rosenwaks, Y. Schottky barrier height and image force lowering in monolayer MoS₂ field effect transistors. *Nanomaterials* **10**, 2346 (2020).
- Dickinson, R. G. & Pauling, L. The crystal structure of molybdenite. *J. Am. Chem. Soc.* **45**, 1466–1471 (1923).
- Zhang, L. et al. Electrochemical ammonia synthesis via nitrogen reduction reaction on a MoS₂ catalyst: theoretical and experimental studies. *Adv. Mater.* **30**, 1800191 (2018).

26. Das, S. et al. Transistors based on two-dimensional materials for future integrated circuits. *Nat. Electron.* **4**, 786–799 (2021).

Acknowledgements

R.K.A.B. acknowledges support from the Stanford Graduate Fellowship (SGF) and the NSERC PGS-D programs. The authors also acknowledge partial support from the SRC SUPREME Center.

Author contributions

R.K.A.B and E.P. conceived the research idea. R.K.A.B. derived and verified the extraction with assistance from L.H. and C.C. R.K.A.B. and E.P. wrote the manuscript with input from all authors. A.J.M. and E.P. supervised the research.

Competing interests

The authors declare no competing interests.

Additional information

Supplementary information The online version contains supplementary material available at <https://doi.org/10.1038/s41699-024-00506-4>.

Correspondence and requests for materials should be addressed to Eric Pop.

Reprints and permissions information is available at <http://www.nature.com/reprints>

Publisher's note Springer Nature remains neutral with regard to jurisdictional claims in published maps and institutional affiliations.

Open Access This article is licensed under a Creative Commons Attribution-NonCommercial-NoDerivatives 4.0 International License, which permits any non-commercial use, sharing, distribution and reproduction in any medium or format, as long as you give appropriate credit to the original author(s) and the source, provide a link to the Creative Commons licence, and indicate if you modified the licensed material. You do not have permission under this licence to share adapted material derived from this article or parts of it. The images or other third party material in this article are included in the article's Creative Commons licence, unless indicated otherwise in a credit line to the material. If material is not included in the article's Creative Commons licence and your intended use is not permitted by statutory regulation or exceeds the permitted use, you will need to obtain permission directly from the copyright holder. To view a copy of this licence, visit <http://creativecommons.org/licenses/by-nc-nd/4.0/>.

© The Author(s) 2025

Supplementary Information

Mobility and Threshold Voltage Extraction in Transistors with Gate-Voltage-Dependent Contact Resistance

Robert K. A. Bennett,¹ Lauren Hoang,¹ Connor Cremers,¹ Andrew J. Mannix,² and Eric Pop^{1,2,3*}

¹*Department of Electrical Engineering, Stanford University, Stanford, CA 94305, U.S.A.*

²*Department of Materials Science and Engineering, Stanford University, Stanford, CA 94305, U.S.A.*

³*Department of Applied Physics, Stanford University, Stanford, CA 94305, U.S.A.*

*Contact: epop@stanford.edu

Supplementary Section 1. Mobility and Threshold Voltage Extraction Tutorial with Accompanying Python Code

We include Python code that automates our extraction procedure, along with I_d vs. V_{ds} data for a sample extraction, in a GitHub Repository.¹ The code is also provided in **Supplementary Section 4**. Here, we provide a tutorial to explain key aspects of this code.

Supplementary Section 1.1. Preliminary Notes and Setting Up

The accompanying code was developed and tested on Python 3.10.12. Running the code requires the following packages: NumPy, statsmodels, and matplotlib (optional, only needed if plotting).

The structure of the code assumes that all I_d vs. V_{ds} sweeps are saved in one central directory. This directory contains one subdirectory for each channel length L_{ch} , where we use the naming convention:

$L_{ch}=X$

where X is the channel length in μm . Each subdirectory contains comma-separated value (csv) files with I_d vs. V_{ds} sweeps at various fixed V_{gs} values using the following naming convention:

$I_dV_d_V_{gs}=Y.csv$

where Y is the fixed V_{gs} value used. Every file contains two column vectors; the first column contains V_{ds} values in units of volts, and the second column contains the corresponding I_d values in units of $\text{A}/\mu\text{m}$. (Here, the current must be normalized by the channel width. Experimental devices must be properly patterned to

prevent errors from current spreading.²⁾ Files are comma-delimited, and the first line of each file is ignored (so that it may be used as a header).

The Python file `VT_mu_extraction.py` contains the functions used in this procedure, and `sample_extraction.py` is a short script that calls these functions on I_d vs. V_{ds} data (we provide sample data in `IdVd_data.zip` in the GitHub Repository¹⁾). Before proceeding, you should download both `.py` files and extract `IdVd_data.zip` (or the appropriate data to be analyzed) to the same directory where the `.py` files are saved. Note that the code assumes that (i) all I_d vs. V_{ds} are forward sweeps, i.e., they are sorted in order of ascending V_{ds} , and (ii) each file contains only one I_d vs. V_{ds} sweep.

Supplementary Section 1.2. Running the Code

The central function that implements the extraction procedure outlined in Figure 2 in the main text, `extraction`, is contained in the module `VT_mu_extraction.py` and called in the script `sample_extraction.py`. To perform the extraction, run the script as provided.

In this script, we set the channel lengths, V_{gs} values, and equivalent oxide thickness (in units of μm , V, and nm, respectively):

```
Lchs = [0.2, 0.4, 0.6, 0.8, 1.0]
vgs_vals = [3.1, 3.2, 3.3, 3.4, 3.5]
EOT = 10
```

We then set the value of I_d^T used in the extraction as $1 \mu\text{A}/\mu\text{m}$ (entered in units of $\text{A}/\mu\text{m}$):

```
IdT = 1e-6
```

The value of I_d^T should be chosen based on your I_d vs. V_{ds} data. As we discuss in the main text, you should choose I_d^T such that all $V_{ds}^{(i)} \ll V_{gs} - V_T$. Typically, we find this condition can be met by taking I_d^T as the I_d for the longest channel device, at the lowest V_{gs} considered, at $V_{ds} \approx 50 \text{ mV}$. To determine if I_d^T is chosen properly, change it by $\sim 25\%$. If the extracted mobility μ or threshold voltage V_T change noticeably, I_d^T is likely too large. Note that the code will throw an error if any I_d vs. V_{ds} sweeps do not reach $I_d = I_d^T$.

The last variable we assign is `NMC`, which is the number of Monte Carlo steps we perform (see **Supplementary Section 2**). We find that typically ~ 1000 Monte Carlo steps is sufficient. As a rule of thumb, the number

of steps is large enough when (i) it is at least 100 and (ii) doubling it does not noticeably change the result of the extraction.

The script uses the following call to assign the extracted μ , the estimated standard error in μ , the extracted V_T , and the estimated standard error in V_T (here, standard error is equivalent to the estimated 68% confidence interval) to the variables `mu_Vds`, `mu_Vds_error`, `VT_Vds`, and `VT_Vds_error`, respectively, and then prints the extracted values to the console:

```
mu_Vds, mu_Vds_error, VT_Vds, VT_Vds_error = extraction(
    foldername_Vds,
    Lchs,
    Vgs_vals,
    EOT,
    IDT,
    NMC,
    plot_Vdsi_extractions = True,
    plot_deltaVC_extractions = True,
    plot_histograms = True)
```

If the last three Boolean variables are `True`, the code will generate and save plots of (i) the L_{ch} vs $V_{ds}^{(i)}$ extraction (similar to Figure 2b in the main text) for every V_{gs} , (ii) extracted voltage drops across the contacts for every V_{gs} (similar to Figure 2c in the main text), and (iii) histograms of distributions from the Monte Carlo procedure, respectively. We recommend inspecting each of these plots to ensure that data was processed correctly and to ensure all extracted quantities make physical sense.

Supplementary Section 2. Monte Carlo Approach for Error Propagation

In our proposed extraction described in the main text, we estimate the intrinsic voltages $V_{ds}'^{(i)}$ and V_{gs}' based on the extracted voltage drop across the contacts, ΔV_C :

$$V_{ds}'^{(i)} = V_{ds}^{(i)} - \Delta V_C \quad (1)$$

$$V_{gs}' \approx V_{gs} - \frac{3}{4} \Delta V_C \quad (2)$$

Here, any uncertainty in ΔV_C will lead to uncertainty in $V_{ds}^{(i)}$ and V_{gs}' that we must propagate throughout the extraction until we eventually apply linear regression to extract V_T and μ in Figure 2e in the main text. Problematically, the errors among data in Figure 2e are not statistically independent from one another, whereas many conventional error estimation methods for linear regression require such independence. As conventional error estimation techniques are therefore inappropriate for estimating uncertainty in our V_T and μ extraction, we instead use the Monte Carlo approach described here to improve our estimates of the nominal V_T and μ and to estimate their uncertainties.

We denote uncertainty in ΔV_C as $\sigma_{\Delta V_C}$. We assume errors in $V_{ds}^{(i)}$ in Figure 2b in the main text are randomly distributed, taking $\sigma_{\Delta V_C}$ as the standard error associated with the y-intercept from linear regression (i.e., the 68% confidence interval). The data points in Figure 2e in the main text (from which V_T and μ are eventually extracted) have error in both their x and y values; we denote these errors as σ_x and σ_y , respectively. We calculate σ_x and σ_y using standard error propagation techniques (implemented in Python code that we have uploaded to a GitHub Repository¹ and included in Supplementary Section 4).

Next, we employ a Monte Carlo approach to simulate how error in ΔV_C propagates to an individual trial when extracting V_T and μ . To do so, we first compile the usual plot in Figure 2e in the main text, denoting the j^{th} x and y pair as $x^{(j)}$ and $y^{(j)}$. Then, for each $x^{(j)}$ and $y^{(j)}$ pair, we:

1. Calculate $\sigma_{\Delta V_C}$ for the $x^{(j)}$ and $y^{(j)}$ pair.
2. Calculate $\sigma_x^{(j)}$ and $\sigma_y^{(j)}$ for the $x^{(j)}$ and $y^{(j)}$ pair.
3. Estimate an adjusted $\tilde{x}^{(j)}$ as a number drawn randomly from a Gaussian distribution with mean $x^{(j)}$ and standard deviation $\sigma_x^{(j)}$.
4. Estimate an adjusted $\tilde{y}^{(j)}$ as a number drawn randomly from a Gaussian distribution with mean $y^{(j)}$ and standard deviation $\sigma_y^{(j)}$.

We then estimate V_T and μ for the Monte Carlo trial (denoted \widetilde{V}_T and $\widetilde{\mu}$) as we do in the main text in Figure 2e: we plot all new $\tilde{x}^{(j)}$ and $\tilde{y}^{(j)}$ pairs, perform linear regression to find the slope \widetilde{m} and the intercept \widetilde{b} , and calculate the V_T and μ for the Monte Carlo trial as $\widetilde{V}_T = \widetilde{m}/2$ and $\widetilde{\mu} = 2I_d^T/(\widetilde{b}C_{ox}W)$.

We repeat this procedure to simulate ~ 1000 distributions of \widetilde{V}_T and $\widetilde{\mu}$. To be consistent with Gaussian statistics (where 68% of data in a normal distribution is within one standard deviation of its median), we take the

standard deviations as half of the range that encompasses 68% of each distribution (centered on the median values), and we take the nominal values as the centers of these ranges.

Supplementary Section 3. Effect of V_T Estimation on TLM Approach for Extracting Mobility

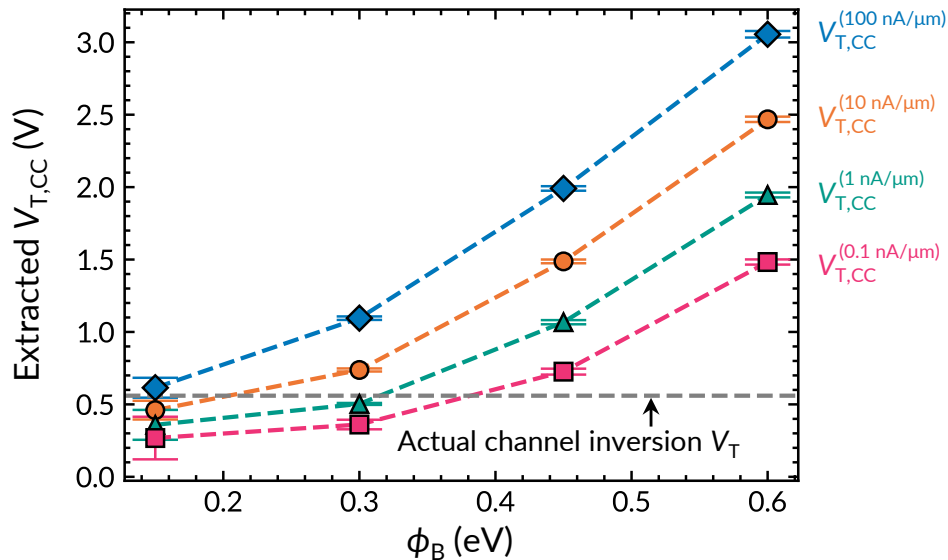
In the transfer length method (TLM) approach^{3,4}, we first measure the I_d vs. V_{gs} characteristics of a family of field-effect transistors (FETs) with different channel lengths (L_{ch}) and estimate the threshold voltage (V_T) for each I_d vs. V_{gs} sweep. Here, we assume such measurements do not have substantial hysteresis,^{4,5} i.e., the change ΔV_T between the forward and backward voltage sweep V_T is negligible. This could be $< 5\%$ of the total overdrive voltage ($V_{ov} = V_{gs} - V_T$) used, i.e., $\Delta V_T/V_{ov} < 0.05$.

Next, we plot I_d vs. V_{ov} for each L_{ch} , find the largest V_{ov} accessible for each device (e.g., if limited by early gate dielectric breakdown), and record the I_d for each device at that common maximum V_{ov} . Using these I_d , we calculate the total resistance $R_{tot} = V_{ds}/I_d$ for each L_{ch} (where V_{ds} is kept small to ensure that the FET operates in the linear regime). We then plot R_{tot} vs. L_{ch} and perform linear regression to find the slope, which is equal to the sheet resistance R_{sh} at that V_{ov} . Finally, we calculate mobility as $\mu = 1/(R_{sh}C_{ox}V_{ov})$.

Because R_{tot} is extracted at a common V_{ov} , the method used to extract V_T influences the estimated μ . In the main text, we use V_T from linear extrapolation for this purpose (at the highest V_{gs} available, i.e., where the channel is most dominant). Here, we repeat extractions using constant-current threshold voltages⁶ $V_{T,CC}$, i.e., the V_{gs} that must be applied to achieve a specified drain current.

We begin by extracting $V_{T,CC}$ for the I_d vs. V_{gs} sweeps in Figures 3a-d in the main text [Schottky barrier height $\phi_B = 0.15$ to 0.6 eV, $L_{ch} = 200$ to 1000 nm, equivalent oxide thickness (EOT) = 10 nm, channel thickness = 0.615 nm, $\mu = 50$ cm²V⁻¹s⁻¹]. Here, we consider $V_{T,CC}$ at constant currents between 0.1 nA/ μ m and 100 nA/ μ m, encompassing the low-power off-current (0.1 nA/ μ m) and high-performance off-current (10 nA/ μ m) specified in the 2022 International Roadmap for Devices and Systems (IRDS).⁷ We plot these $V_{T,CC}$ in **Supplementary Figure 1**.

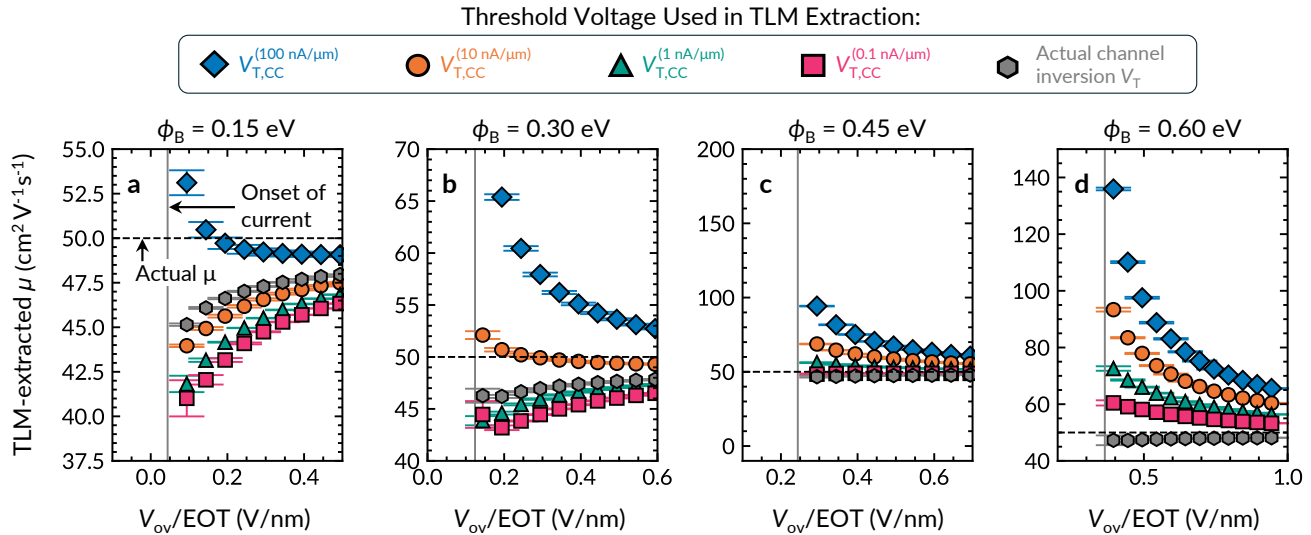
Next, we repeat the TLM μ extraction presented in the main text, this time extracting R_{tot} at a common $V_{ov} = V_{gs} - V_{T,CC}$ using the $V_{T,CC}$ plotted above. For comparison, we also extract μ from the TLM method using the true channel inversion V_T , which is known *a priori* for our TCAD-generated I_d vs. V_{gs} data (but is difficult to determine for experimental contact-gated FETs, as we discuss in the main text).



Supplementary Figure 1: Constant-current threshold voltages $V_{T,CC}$ from I_d vs. V_{gs} curves in Figures 3a-d of the main text. Error bars show the range of $V_{T,CC}$ extracted from $L_{ch} = 200$ to 1000 nm. In labels, superscripts denote the current at which $V_{T,CC}$ was extracted. The horizontal dashed line marks the true channel inversion V_T .

As shown in **Supplementary Figure 2**, using the true channel inversion V_T allows the TLM approach to accurately extract the μ with $< 10\%$ error even in strongly contact-gated devices. This result suggests that the TLM approach fails in contact-gated devices in the main text due to V_T estimation error propagating to the extracted μ . We also find that when using $V_{T,CC}$, the accuracy of the TLM approach depends on the current at which $V_{T,CC}$ is extracted. When $V_{T,CC}$ happens to be close to the channel inversion V_T (see Supplementary Figure 1), the TLM approach becomes accurate. We also note that the error in the extracted μ decreases at higher V_{ov} , which occurs because errors in V_T have a larger impact on V_{ov} when V_{ov} itself is small. (If the error in V_T is ΔV_T , the relative error in V_{ov} is $\delta V_{ov} = |\Delta V_T / V_{ov}| = |\Delta V_T / (V_{gs} - V_T)|$, which tends to 0 as V_{gs} increases.)

The above analysis suggests that the TLM approach can be suitable when the channel inversion V_T can be accurately determined; however, as we discuss in the main text, extracting this V_T from I_d vs. V_{gs} characteristics of contact-gated devices remains challenging. (Additionally, even with the correct V_T , error bars still do not accurately reflect the true uncertainty in the TLM-extracted μ .) Our results indicate that $V_{T,CC}$ taken at $0.1 \text{ nA}/\mu\text{m}$ generally allows for the TLM method to accurately extract μ for the transistors we investigate in this work; however, the current at which $V_{T,CC}$ matches the channel inversion V_T can vary significantly depending on device specifics. Thus, we caution against assigning a universal common $V_{T,CC}$ for μ extraction using the TLM approach.



Supplementary Figure 2: Impact of V_T extraction on TLM approach accuracy. Mobility μ extracted using the TLM approach for families of devices with contact Schottky barrier $\phi_B =$ (a) 0.15 eV, (b) 0.3 eV, (c) 0.45 eV, and (d) 0.6 eV. We use various extracted constant-current threshold voltages $V_{T,CC}$ and the true channel inversion V_T to benchmark devices at a common overdrive V_{ov} while estimating R_{ot} for the TLM extraction. Different markers indicate which $V_{T,CC}$ was used for this purpose, as denoted in the legend. The horizontal dashed lines mark the actual μ . The gray vertical lines mark the approximate V_{ov} where each family of devices begins to turn on in their I_d vs. V_{gs} characteristics (same as the vertical lines in Figure 3 in the main text).

Supplementary Section 4. Python Code to Automate the Proposed Extraction

At the end of this Supplementary Information, we provide Python code to automate the extraction proposed in this work. An up-to-date version of this code and a sample dataset for the extraction can also be found in an online GitHub repository.¹ See Supplementary Section 1 for a tutorial on how to run this code and for a description of how the current vs. voltage data should be formatted.

Supplementary References

- 1 Bennett, R.K.A. *GitHub Repository*. Available online: github.com/RKABennett/VT_mu_extraction.
- 2 K orođlu,  . *et al.* Fringe current correction for unpatterned-channel thin-film transistors including contact resistance and velocity saturation effects. In review (2024).
- 3 Cheng, Z. *et al.* How to report and benchmark emerging field-effect transistors. *Nature Electronics* **5**, 416-423, doi:10.1038/s41928-022-00798-8 (2022).
- 4 Das, S. *et al.* Transistors based on two-dimensional materials for future integrated circuits. *Nature Electronics* **4**, 786-799, doi:10.1038/s41928-021-00670-1 (2021).
- 5 Datye, I. *et al.* Reduction of hysteresis in MoS₂ transistors using pulsed voltage measurements. *2D Materials* **6**, 011004, doi:10.1088/2053-1583/aae6a1 (2019).
- 6 Ortiz-Conde, A. *et al.* Revisiting MOSFET threshold voltage extraction methods. *Microelectronics Reliability* **53**, 90-104, doi:10.1016/j.microrel.2012.09.015 (2013).
- 7 IEEE. International Roadmap for Devices and Systems – More Moore. Accessed: 2024 April 18. Available online: <https://irds.ieee.org/editions/2022/more-moore> (2022).

```

from math import sqrt
import matplotlib as mpl
import matplotlib.pyplot as plt
import numpy as np
import random
import os
import sys
from VT_mu_extraction import extraction

# get the current working directory
dir_path = os.path.dirname(os.path.abspath(__file__))
sys.path.append(dir_path + '/../')

data = dir_path + '/IdVd_data'           # directory with Id vs. Vds data
Lchs = [0.2, 0.4, 0.6, 0.8, 1.0]        # channel lengths in um
vgs_vals = [3.1, 3.2, 3.3, 3.4, 3.5]    # gate voltages in V
EOT = 10                                # equivalent oxide thickness in nm

np.random.seed(0) # seed for reproducibility

IDT = 1e-6
NMC = 500

mu, mu_error, VT, VT_error = extraction(
    data,
    Lchs,
    vgs_vals,
    EOT,
    IDT,
    NMC,
    plot_Vdsi_extractions = True,
    plot_deltaVC_extractions = True,
    plot_histograms = True,
)

print ('Estimated_mobility:_{ }_cm^2_V^s-1_S^-1'.format(mu))
print ('Estimated_mobility_error:_{ }_cm^2_V^s-1_S^-1'.format(mu_error))
print ('Estimated_VT:_{ }_V'.format(VT))
print ('Estimated_VT_error:_{ }_V'.format(VT_error))

```

```

from math import sqrt
import matplotlib as mpl
import matplotlib.pyplot as plt
import numpy as np
import os
import random
from pathlib import Path
import statsmodels.api as sm

# get the current working directory
dir_path = os.path.dirname(os.path.abspath(__file__))

def extraction(
    foldername,
    Lchs,
    Vgs_vals,
    EOT,
    IDT,
    NMC,
    plot_Vdsi_extractions = False,
    plot_deltaVC_extractions = False,
    plot_histograms = False
):
    '''
    Applies the method in [CITATION] on Id vs. Vds data to extract the mobility
    and threshold voltage of contact-gated FETs. Mentions of equations,
    figures, variables, etc can be found in the above reference.

    Keyword arguments:
    foldername -- Directory where Id vs. Vgs sweeps are stored
    Lchs       -- Array-like object listing out channel lengths used
                (units: um)
    Vgs_vals   -- Array-like object listing out Vgs values used
                (units: V)
    EOT       -- Equivalent oxide thickness (units: nm)
    IDT       -- I_d`T value used for constant-current extraction
                (units: uA or uA/um (should be the same as the units
                for Id)
    NMC       -- Number of Monte Carlo trials used for error prop
                (Tip: make sure NMC is large enough by
                increasing it to ensure that doing so does not
                change the final extracted values)

    Returns:
    mu        -- Channel mobility (units: cm^2 V^-1 s^-1)
    mu_err    -- Estimated standard error for mu
                (units: cm^2 V^-1 s^-1)
    VT       -- Channel inversion threshold voltage (units: V)
    VT_err    -- Estimated standard error for VT (units: V)
    '''

    if plot_Vdsi_extractions or plot_deltaVC_extractions or plot_histograms:
        Path(dir_path + '/plots').mkdir(parents=True, exist_ok=True)
        # plot settings
        mpl.rcParams['lines.linewidth'] = 1.5
        mpl.rcParams['axes.linewidth'] = 0.9
        mpl.rcParams['xtick.major.width'] = 0.6
        mpl.rcParams['ytick.major.width'] = 0.6
        mpl.rcParams['xtick.minor.width'] = 0.3
        mpl.rcParams['ytick.minor.width'] = 0.3
        mpl.rcParams['font.family'] = 'arial'
        plt.rcParams['xtick.minor.visible'] = True
        plt.rcParams['ytick.minor.visible'] = True
        plt.rcParams["xtick.top"] = True
        plt.rcParams["ytick.right"] = True
        mpl.rcParams['xtick.direction'] = 'in'
        mpl.rcParams['ytick.direction'] = 'in'
        plt.rcParams.update({'font.size': 16})

    #####
    #
    # Compile a table of Vds' and Vgs' values similar to that of Fig. 2e in the
    # main text
    #
    #####

    data_list = []

    # Extract Vds' and Vgs' values for every Vgs
    for Vgs in Vgs_vals:
        Vdsi_list,\

```



```

Vch_list,\
Vgsp,\
error_VC = extract_at_fixed_Vgs(
                                foldername,
                                Lchs,
                                Vgs,
                                IDT,
                                plot_deltaVC_extractions,
                                plot_Vdsi_extractions
                                )

data_list.append([Vdsi_list, Vch_list, Vgsp, error_VC])

# Now, we iterate through each channel length. We use our extracted Vgsp
# values in conjunction with the appropriate Vdsp values to come up with
# our x and y values, and their accompanying errors, for the final fit.
# Here, x and y values are those plotted on the x- and y-axes in Fig. 2e.

xy_mat = build_data_matrix(Lchs, Vgs_vals, data_list)

#####
#
# Perform multiple Monte Carlo iterations to simulate distributions of mu
# and VT based on their estimated errors
#
#####

mu_list, VT_list, x, y, x_error, y_error = [], [], [], [], [], []

for i in range(NMC):
    mu_i, VT_i = MC_step(xy_mat, EOT, IDT)

    mu_list.append(mu_i)
    VT_list.append(VT_i)

#####
#
# Extract the nominal mobility/VT and their accompanying standard errors
#
#####

mu_list = np.sort(mu_list)
VT_list = np.sort(VT_list)
x = np.array(x)
y = np.array(y)

# Here, we filter the histograms by taking the median value +- 34% (i.e.,
# the central 68% of the histograms) to stay roughly in line with Gaussian
# statistics, as we discuss in the Supporting Information.

p1 = 16 # exclude the bottom 16% of the histogram
p2 = 100-p1 # exclude the top 16% of the histogram

mu_filtered = mu_list[
    int(np.size(mu_list)* p1/100)
    :
    int(np.size(mu_list)* p2/100)
]

VT_filtered = VT_list[
    int(np.size(VT_list)* p1/100)
    :
    int(np.size(VT_list)* p2/100)
]

# Uncomment the following lines to plot histograms of mu and VT before
# and after filtering. (It's normal for unfiltered distributions to contain
# extreme outliers. This is one of the reasons why we filter.)

# Calculate and return the final mu and VT values
mu = (mu_filtered[0] + mu_filtered[-1])/2
mu_error = (mu_filtered[-1] - mu_filtered[0])/2
VT = (VT_filtered[0] + VT_filtered[-1])/2
VT_error = (VT_filtered[-1] - VT_filtered[0])/2

if plot_histograms:
    histogram_fit(mu_list, 2, foldername, 'mobility')
    histogram_fit(mu_filtered, 2, foldername, 'mobility_filtered')
    histogram_fit(VT_list, 0.2, foldername, 'VT')
    histogram_fit(VT_filtered, 0.2, foldername, 'VT_filtered')

```

```

return mu, mu_error, VT, VT_error

def extract_at_fixed_Vgs(foldername, Lchs,
                        Vgs, IDT, plot_deltaVC_extractions,
                        plot_Vdsi_extractions):
    '''
    Extracts the voltage drop across the channel, Vch, for an Id vs. Vds sweep
    at a fixed target current = Id^T.

    Keyword arguments:
    foldername      -- Directory where Id vs. Vgs sweeps are stored
    Lchs            -- Array-like object listing out channel lengths used
                    (units: um)
    Vgs            -- Vgs value at which Id vs. Vds sweep is performed
    IDT            -- Id^T value used for constant-current extraction
                    (units: uA or uA/um (should be the same as the units
                    for Id))

    Returns:
    Vdsi_list       -- List containing the Vds^(i) value for each Lch
    Vdsip_list      -- List containing Vds^(i)' values for each Lch
    Vgsp           -- Vgs'
    error_delta_VC -- Estimated standard error in delta V_C
    '''

    Vdsi_list = find_Vds_list(foldername, Lchs, Vgs, IDT, plot_Vdsi_extractions)
    Lchs = np.array(Lchs, dtype = 'float64')

    #####
    #
    # Statistics to find b, m, and the error for b
    #
    #####

    x = Lchs
    x = sm.add_constant(x)
    y = Vdsi_list

    delta_VC, m, error_delta_VC, error_m = linear_regression(x,y)
    Vdsip_list = Vdsi_list - delta_VC # List of Vds^(i)'
    Vgsp = Vgs - 0.75*delta_VC # Vgs'

    #####
    #
    # Optional: uncomment this section to generate a TLM-like plot (same as
    # in Fig. 2b) for the delta V_C extraction.
    #
    #####

    if plot_deltaVC_extractions:
        Path(dir_path + '/plots/deltaVC_extractions').mkdir(
            parents=True,
            exist_ok=True)

        plotname = '/deltaVC_extraction_Vgs={}.png'.format(Vgs)
        x = np.array([0, np.max(Lchs)])
        y = m*x + delta_VC

        fig, ax = plt.subplots(1,1)

        ax.plot(
            Lchs,
            Vdsi_list*1000,
            marker = 'o',
            color = 'k',
            ls = 'None'
        )

        ax.plot(
            x,
            y*1000,
            color = 'r',
            ls = '--',
            marker = 'None'
        )

        ax.set_xlim(0,)
        ax.set_xlabel('$L_{\mathrm{ch}}$ (um)')
        ax.set_ylabel('$V_{DS}_{\mathrm{at}}$ (mV) at $I_{d_{\mathrm{T}}}$')
        plt.tight_layout()
        plt.savefig(dir_path + '/{}/{}'.format(
            'plots/deltaVC_extractions',

```

```

                                plotname)
                                )
plt.close()

return(Vdsi_list, Vdsip_list, Vgsp, error_delta_VC)

def find_Vds_list(foldername, Lchs,
                 Vgs, IDT, plot_Vdsi_extraction):
    '''
    Finds the Vds values where Id = some target current for a family of IdVd
    curves at different Lchs.

    Keyword arguments:
    foldername      -- TBA
    Lchs            -- Array-like object listing out channel lengths used
                    (units: um)
    Vgs             -- Vgs value at which Id vs. Vds sweep is performed
    EOT            -- Equivalent oxide thickness (units: nm)
    IDT            -- I_d^T value used for constant-current extraction
                    (units: uA or uA/um (should be the same as the units
                    for Id))

    Returns:
    Vdsi_list       -- List of V_ds^(i) values for each Lch values
    '''

    basefilename = foldername + '/Lch={}/IdVd_Vgs={}.csv'
    if plot_Vdsi_extraction:
        Path(dir_path + '/plots/Vdsi_extractions').mkdir(parents=True,
                                                         exist_ok=True)

        fig, ax = plt.subplots(1,1)

    for Lch in Lchs:
        data = np.loadtxt(
            basefilename.format(Lch, Vgs),
            skiprows = 1,
            delimiter = ',',
            ).T

        Vd = data[0]
        Id = data[1]

    Vdsi_list = []

    for Lch in Lchs:
        data = np.loadtxt(
            basefilename.format(Lch, Vgs),
            skiprows = 1,
            delimiter = ',',
            ).T

        Vd = data[0]
        Id = data[1]
        Vds_target = find_Vds_targ(Vd, Id, IDT)
        Vdsi_list.append(Vds_target)

    if plot_Vdsi_extraction:
        ax.plot(
            Vd*10**3,
            Id*10**6,
            label = Lch
        )
        ax.plot(
            Vds_target*10**3,
            IDT*10**6,
            marker = 'o',
            color = 'k',
        )
        ax.axhline(IDT*10**6, ls = '--', color = 'k')

    if plot_Vdsi_extraction:
        ax.set_ylim(0, 2*IDT*10**6)
        ax.set_xlim(np.min(Vd)*10**3, 1.1*np.max(Vdsi_list)*10**3)
        ax.set_xlabel('$V_{\mathrm{ds}}$ (mV)')
        ax.set_ylabel('$I_{\mathrm{d}}$ (uA/um)')
        ax.legend(loc = 'best', title = '$L_{\mathrm{ch}}$')
        plt.title('$V_{\mathrm{gs}}$ + str(Vgs) + 'uV')
        plt.tight_layout()
        plt.savefig(dir_path + '/{}/Vdsi_extraction_Vgs={}.png'.format(
            'plots/Vdsi_extractions',
            Vgs))

    plt.close()
    return np.array(Vdsi_list)

```

```

def find_Vds_targ(Vds, Id, IDT):
    """
    Finds the Vds value of a single IdVd where Id = some target current.

    Keyword arguments:
    Vds and Id      -- Array-like objects of V_ds and I_d values used in
                    Id vs. Ids sweep (units: V_ds in V; Id in uA or uA/um)
    EOT             -- Equivalent oxide thickness (units: nm)
    IDT             -- I_d^T value used for constant-current extraction
                    (units: uA or uA/um (should be the same as the units
                    for Id))

    Returns:
    Vds_target      -- Vds value at which Id = target current (same as V_ds^(i)
                    in the main text)

    Note that if Vds_target is between two values (which is usually will be),
    we perform linear extrapolation using the two neighboring datapoints. If
    the Id vs. Vds sweep contains multiple Vds values corresponding to the
    chosen IDT (which can happen if you have multiple sweeps in
    your curve or if you have noise), then we return only the first.
    """

    for i in range(np.size(Vds) - 1):
        if (
            (Id[i] < IDT and Id[i + 1] > IDT)
            or Id[i] == IDT
        ):
            m = (Id[i+1] - Id[i]) / (Vds[i+1] - Vds[i])
            b = Id[i] - m*Vds[i]
            Vds_target = (IDT - b)/m
            return Vds_target

    raise Exception("Could_not_find_Vdsi_value._Was_your_IDT_chosen_properly?")

def MC_step(xy_mat, EOT, IDT):
    """
    Implements a single step of the Monte Carlo method (see Section S2). We
    call this function many times to build up distributions of mu and VT that
    we then process to find better estimates for their nominal values and
    corresponding errors.

    xy_mat:        -- matrix generated using 'build_data_matrix' function
    EOT            -- Equivalent oxide thickness (units: nm)
    IDT            -- I_d^T value used for constant-current extraction
                    (units: uA or uA/um (should be the same as the units
                    for Id))

    Returns:
    mu             -- mobility from a single Monte Carlo step (equivalent to
                    \tilde{\mu} in Section S2 of the Supporting Information)
    VT            -- Threshold voltage from a single Monte Carlo step
                    (equivalent to \tilde{V_T} in Section S2 of the
                    Supporting Information)
    """
    # unpack the xy_mat for convenience
    xval          = xy_mat[:,0]
    error_x       = xy_mat[:,1]
    yval          = xy_mat[:,2]
    error_y       = xy_mat[:,3]
    error_b       = xy_mat[:,4]

    # lists that we will populate with x and y values (as in Fig. 2e) for our
    # eventual linear regression.
    x = []
    y = []

    # apply the method described in Section S2 of the supporting information to
    # generate a series of perturbed x and y data points
    for j in range(np.size(xval)):
        error_in_b1 = np.random.normal(0,error_b[j],1)[0]
        error_in_x  = error_in_b1 * abs(error_x[j])
        error_in_b2 = np.random.normal(0,error_b[j],1)[0]
        error_in_y  = error_in_b2 * abs(error_y[j])
        new_xval    = xval[j] + error_in_x
        new_yval    = yval[j] + error_in_y
        x.append(new_xval)

```

```

        y.append(new_yval)

b, m, b_error, m_error = linear_regression(x,y)

Cox = 8.85e-12*3.9/(EOT*10**-9)
A = (10**4/Cox*2*IDT)

# extract the mobility and VT for the single Monte Carlo trial
mu = A/b
Vth = m/2
return mu, Vth

def build_data_matrix(Lchs, Vgs_vals, data_list):
    '''
    Builds a matrix containing [xvals, xerrs, yvals, yerrs, error_VCs]
    where:
        xvals          -- nominal x values in Fig. 2b
        xerrs          -- error bars prefactor for x values in Fig. 2b
        yvals          -- nominal y values in Fig. 2b
        yerrs          -- error bars prefactor for y values in Fig. 2b
        error_VC       -- error in delta VC

    Here, xerrs and yerrs are prefactors, i.e., they must be multiplied by
    error_VC to get the true error in the x and y values. Thus, xerr and yerr
    are equivalent to the quantities described in equations S3 and S4 divided
    by sigma_V_C.

    Keyword arguments:
    Lchs              -- Array-like object listing out channel lengths used
                       (units: um)
    Vgs_vals          -- Array-like object listing out Vgs values used
                       (units: V)
    data_list         -- Matrix-like object built using the
                       'extract_at_fixed_Vgs' function

    Returns:
    xy_mat            -- The matrix described above
    '''
    xy_mat = []
    for j in range(len(Lchs)):
        Lch = float(Lchs[j])
        for i in range(len(Vgs_vals)):
            Vdsi_list, Vch_list, Vgsp, error_b = data_list[i]
            Vdsp = Vch_list[j]

            A = 2*Vgsp*Vdsp
            B = Vdsp**2

            errorA = A*sqrt((3/4 / Vgsp)**2 + (1 / Vdsp)**2)
            errorB = B*sqrt(2*(1 / Vdsp)**2)

            error_x = 1 / Lch
            error_y = np.sqrt(errorA**2 + errorB**2)/Lch

            xval = Vdsp/Lch
            yval = (2*Vgsp*Vdsp - Vdsp**2)/Lch

            xy_mat.append([xval, error_x, yval, error_y, error_b])

    return np.array(xy_mat)

def histogram_fit(vals, step,
                  savefoldername, hist_name):
    '''
    Generates and saves a histogram to visualize mu or VT distributions
    obtained from the Monte Carlo procedure.

    Keyword arguments:
    vals              -- quantities of interest (mu or VT values) whose distribution
                       you want to see
    step              -- step size for bins
    foldername        -- directory to which you wish to save the histogram
    hist_name         -- file name for saving

    Returns:
    N/A
    '''
    Path(dir_path + '/plots/histograms').mkdir(parents=True, exist_ok=True)
    fig, ax = plt.subplots(1,1)
    bins = np.arange(np.min(vals), np.max(vals) + 2*step, step)

```

```

ax.hist(vals, edgecolor = 'k', color = 'gray', bins = bins)
ax.set_xlim(np.min(vals), np.max(vals))
ax.set_title('Min={}, max={}, range={}'.format(
    round(vals[0], 2),
    round(vals[-1], 2),
    round(vals[-1] - vals[0], 2)
))
ax.set_xlabel('Value')
ax.set_ylabel('Count')
plt.tight_layout()
plt.savefig(dir_path\
    + '/plots/histograms/histogram_{}.png'.format(hist_name))
plt.close()

def linear_regression(x, y):
    """
    Implements linear regression for a collection of x,y data.

    Keyword arguments:
    x          -- Array-like object of independent variable
    y          -- Array-like object of dependent variable

    Returns:
    b          -- y-intercept for line of best fit
    m          -- Slope of line of best fit
    b_error    -- Standard error for y-intercept
    m_error    -- Standard error for slope
    """
    X = sm.add_constant(x)
    model = sm.OLS(y, X).fit()
    results_summary = model.summary()
    b = model.params[0]
    m = model.params[1]
    b_error = model.bse[0]
    m_error = model.bse[1]

    return b, m, b_error, m_error

```